arXiv:astro-ph/9610207v1 25 Oct 1996

Detailed lensing properties of the MS2137-2353 core and reconstruction of sources[1]

F. Hammer and P. Teyssandier

DAEC, Observatoire de Paris-Meudon, 92195 Meudon, France

E. J. Shaya

University of Maryland, Dept. of Physics, College Park, MD 20742

I. M. Gioia[2] and G. A. Luppino

IfA, University of Hawaii, USA

and

O. Le Fèvre

DAEC, Observatoire de Paris-Meudon, 92195 Meudon, France

Received ____________________; accepted ____________________

---

[1]Based on observations made with the NASA/ESA Hubble Space Telescope, obtained at the Space Telescope Science Institute, which is operated by AURA under NASA contract NAS5-26555

[2]Also Istituto di Radioastronomia del CNR, Via Gobetti 101, I-40129, Bologna, ITALY

ABSTRACT

A deep HST image of the MS 2137-2353 core has revealed detailed morphological structures in two arc systems, which are modelled and well reproduced after a complete analysis of the lensing properties of the dark matter component. Latter could have a simple elliptical mass distribution with ellipticity and angular orientation similar to those of the visible and X-ray light, which suggests that the MS 2137-2353 is a relaxed cluster at z=0.313. The predicted density profile ($\rho \sim r^{-1.56\pm0.1}$ with $r_c \leq 22.5 h_{50}^{-1}$ kpc) within $150 h_{50}^{-1}$ kpc implies increasing M/L ratio with the radius, and could be in agreement with predictions from standard CDM simulations.

At least two faint sources (unlensed magnitude, R=23.9 and 26, respectively) are aligned with the cluster core and are responsible of the arc systems. They have been reconstructed with details as small as 0".02 (or $160 h_{50}^{-1}$ pc in the source assumed at z= 1), one could be a nearly edge-on barred spiral galaxy, and the other has a more complex morphology, which could be related to a close interacting pair and/or to dust. They show strong signs of star formation indicated by compact HII regions well off their center. The observation of giant luminous arcs by HST could even resolve the size of giant HII regions at z$\sim$ 1.

Subject headings: clusters: galaxies, cosmology: gravitational lensing - dark matter

Subject headings: clusters: galaxies, cosmology

1. Introduction

A large number of giant luminous arcs have been discovered in the cores of rich clusters of galaxies (e.g. Fort and Mellier, 1994). They provide the best estimates of the mass within few hundred of kpc of the cluster center. However, ground based images generally do not allow one to resolve the arc widths and structures, leading to a considerable uncertainty on both the shape of the density profile and the magnification factor (Hammer, 1991). Statistical approaches partially remove the uncertainty on the density profile and the number of arcs discovered is consistent with very small core radii ($r_c < 50\ h_{50}^{-1}$ kpc) in most of the arc clusters (Wu and Hammer, 1993). This is supported by the discovery of the so-called radial arcs, which require small core radius for the lensing cluster (Mellier et al, 1993).

There is an increasing interest to understand the dynamics of the most inner part of the clusters. In the framework of the standard CDM cosmogony, N-body simulations have predicted singular density profiles, approaching the halo center with $\rho \sim r^{-1}$ (Navarro et al, 1995; Tormen et al, 1996). It has been argued that the presence of radial arcs in cluster cores was consistent with such "universal" dark-matter halo profile (Baltermann, 1996) as well as with isothermal mass profile ($\rho \sim r^{-2}$) with small and definite core.

The 0".1 pixel size of the WFPC2 of the Hubble Space Telescope allows the resolution of most of the giant luminous arcs, which leads to considerable constraints on both the cluster core mass distribution and on the source morphology. In this letter we analyse the lensing properties of the MS 2137-2353 core in which two multiple image systems have been discovered so far (Fort et al, 1992), and which have been observed by the HST (Gioia et al, 1996a). Throughout the paper, values of H_0=50 and q_0=0.5 are assumed.

2. Image analysis

2.1. Arc templates

Before modelling, arc images should be cleaned from the contamination due to the cluster galaxy light, especially the brightest cluster galaxy G1 and the galaxy G7 which is superimposed to the edge of the giant arc. Arc template images used to feed the lensing model have been also limited above the threshold of 1σ above the average background noise. The standard package STSDAS (task ellipse) in IRAF has been used to model the contaminating galaxies G1, G7 and the four small galaxies lying within the envelope of G1. Figure 1 shows the cluster core after removing the background and the contaminating galaxies G1 and G7. Within the envelope of G1, the residual noise is 1.5 to 3 times higher than the background sky noise. We find no evidence for a fifth image which could be associated to the arc system (A0, A2 and A4). The radial arc (AR) extends from 3".4 to 7".0 from the mass center and is surrounded by a rather complex structure.

2.2. Optical properties of the cluster

The brightest cluster galaxy G1 is well fitted by an ellipse with ellipticity varying from 0.12±0.02 in the very center (r=2") to 0.16±0.02 beyond r=6" (or $34h_{50}^{-1}$ kpc) and P.A.= 47.5±5 degrees (the header keyword ORIENTAT of the HST image is 142.5). Both ellipticity and P.A. of G1 are in rather good agreement with values derived from the X-ray gas (ϵ=0.13±0.02 and P.A.=65±15 degrees, Gioia et al, 1996a). Its surface brightness profile does not follow a $r^{1/4}$ law, while it shows a rather steep profile beyond r=3" (β=1.6 for $\sigma\sim (1+(r/r_c)^2)^{0.5-\beta}$). The latter number is derived from the output of the task ellipse (package STSDAS). The HST image quality reveals that the galaxy G7 is a nearly edge-on spiral galaxy (axis ratio=0.54) with a nicely defined bulge (it is probably an Sa).

3. Lensing model and methodology

Gravitational bending angles can be computed for various sets of mass density profiles in the code AIGLE (Astronomical Instrument for Gravitational Lensing Experiments). It is an up-dated version of the code written by Hammer and Rigaut (1989) and includes inversion of the lensing equation through the Schramm and Kayser (1987) method. Elliptical lenses are assumed to follow the homoeidal mass distribution (see Schramm, 1990) and the projected isodensities are concentric ellipses, with various density profiles. Mass distribution are used as input of the code rather than potential. Several techniques have been implemented to optimise the modelling, including χ^2 tests for the comparison between the arc fit and the arc template, and self consistency and coherence tests for the source reconstruction in the case of multiple image configuration (see e.g Wallington et al, 1995). For a system with four images of the same source, the basic methodology to model the arcs consists of the following three steps : (i) to invert the lensing equation for a given sub-structure (generally the brightest knot) of the source, to compare the fit to the observations and to optimise it, and hence, to investigate the degeneracy of the parameters; (ii) to reconstruct the source for each the 4 individual images and test the consistency between the 4 reconstructed source images (RSIs); (iii) to combine the RSIs and to reconstruct the source of the system, and by using the most self consistent reconstructions, to invert again the lensing equation and to test the result by comparison with the arc templates. The latter test securely ensures that the reconstructed source is not providing extra-images which are not observed.

4. Model of the arcs

We have assumed a single β profile model (ρ=ρ_0 $(1 + (r/r_c)^2)^{-\beta}$) for the cluster core, and have investigated the space of the mass parameters (P.A., ϵ, r_c, β and σ^2) to reproduce

the arc location. Source reconstruction is then derived and self consistency tests are applied. We finally consider perturbations from the secondary deflectors (such as G1 and G7) and discuss them. Examination of the arc templates confirms the identification of one multiple image system which is composed of 4 images (A01, A02, A2 and A4) of a single source (S1). No evidence is found for a fifth image near the center of G1, which suggests that it is actually overfocused (low magnification factor). The other system is made of 3 images (A6 and AR) of a second source (S2), the radial arc being a complex mix of two images.

4.1. Images A01, A02, A2 and A4 of the S1 source

For a large variety of sets of mass parameters, we have been able to reproduce the location of the brightest knot in each of the four images, within 1 pixel accuracy. The P.A. of the lens major axis is well constrained within 41-46 degrees, in rather good agreement with both optical and X-ray light. There is an obvious degeneracy between the other parameters, which is illustrated in Figure 2. Assuming a value for r_c and ϵ (>0.06) generally provide a solution which set β and the mass (proportional to the square of the line of sight velocity dispersion, σ_{los}). Values for the latter do not differ from the ones found by Mellier et al (1993), for β=1 and r_c=7" (for which we find σ_{los}=1216kms^{-1} if the source is assumed at z=1), and differences between mass estimations from lensing and from X-ray measurements are discussed by Gioia et al (1996a). We have mapped the (r_c, ϵ) plane assuming several values for β. For each set of parameters (r_c, ϵ and β), we have calculated the 4 reconstructed source images (RSIs) corresponding to the 4 arcs (A01, A02, A2 and A4), assuming a pixel size in the source plane of 0".02 (Figure 3). It results that the arc A0 is a double image of only a fraction of the source, because the source is superimposed on to the diamond shape caustic line. This is a good illustration of the predictive model for an elliptical lens made by Bourassa and Kantowski (1975). To test the consistency (or

similarity) between the 4 RSIs, we have calculated the angular distances from the brightest knot to 2 other knots found in the RSI of A01 and A02, and to 4 other knots found in the RSI of A2 and A4 (see Figure 3). The self similarity parameter is defined as:

$$\mathrm{SSP} = \Sigma_k \, \Sigma_{i>j} |d(A_i, k)/d(A_j, k) - 1|/6,$$

where the summations have been done on the knots (k), the RSIs (i), and the angular distance between the brightest knot and the knot (k) in the RSI (i) is $d(A_i, k)$. Values of SSP are indicated in Figure 2, and typical error bars are $\pm$ 0.08. It takes minimal values ($\sim$ 0.3) for β ranging between 0.6 to 0.85, leading to ellipticities ranging from 0.06 to 0.18 and core radius lower than 8". β=1 profiles imply too large sizes for the RSIs of A4, A01 and A02 compared to the RSI of A2. Steeper mass profiles (β=1.5) provide even more implausible solutions. Figure 3 shows one of the best reconstruction which corresponds to one of the minimum value for the self similarity parameter (SSP =0.35 with β=0.8, r_c=2 and ϵ=0.151). The reconstructed source images (RSIs) show very nice consistency, especially when one accounts for the fact that the RSIs of A01 and A02 are only sampling a small (top-left) part of the source. Both the noise and artifacts are damped when the RSIs are combined, providing a detailed image of the actual source (S1) of this arc system (Figure 3, middle panel). Other best reconstructions of the source present very similar morphology and only the source size is affected, which corresponds to variation in the magnification factor. The simulated arcs can be rebuilt by re-imaging the reconstructed source by the model, and can be compared to the observed one (Figure 1). Again, the similarity between the simulation and the actual arc images is very good, even in the small details.

There are however some discrepancies between the 4 reconstructed source images (RSIs). Also our investigation of a large fraction of the parameter space has not provided a solution with a self similarity parameter (SSP) very close to 0. We believe that several reasons can explain these residual discrepancies: (i) the mass profile is too naive and β is

varying with the radius; (ii) there are perturbations by secondary lenses (cluster galaxies); (iii) there might be an additional elliptical component with a different orientation than the main one; (iv) the compactness of some knots (such as the brightest one), provides artificial elliptical shapes in the RSIs; (v) we suspect that one faint knot in the arc A2 is a contaminating object. We have tested the influence of G7 as a secondary lens. Acceptable mass values for G7 (which corresponds to σ=120kms^{-1} for an isothermal profile) are equal or below 1% of the cluster core mass, and slightly affect the predicted parameters for the cluster mass distribution (for example it decreases the ellipticity by $\sim$ 10%). The problem associated with larger values for the G7 mass, is that they imply too large sizes for the reconstructed source image (RSI) of A02 (compared to the RSI of A2), and degrade significantly the source reconstruction (σ > 150 kms^{-1} for G7 is rejected at a 3σ level).

4.2. Images A6 and AR (radial arc) of the source S2

To model this arc system, we have tested each of the parameter sets which reproduce the arc location in the formerly discussed arc system (A0, A2 and A4, see Figure 2). The extension of the radial arc very close to the mass center (3".4) implies very small values for the core radius r_c (< 3".5 for β=0.8). Figure 2 shows the available range of parameters which can reproduce the radial arc location (left side of the dotted line). For this range of parameters, the source (of A6 and AR) should have a redshift very similar to that of the source (S1) of A0, A2 and A4 (assuming z=1 for the latter implies $1 \leq z \leq 1.03$ for the former). The source (S2) has a morphology which can be suggestive of a nearly edge-on barred spiral (Figure 3) with rather asymetric arms. The radial arc is most likely a blended image of the bar, almost aligned towards the mass center (as the radial arc). A re-imaging of the source S2 is presented in Figure 1, and well reproduces the length and the location of the radial arc. However it cannot reproduce the bright knot 1".4 above AR, which should

be related to another system. We found that this knot could be an additional image of the A5 source (S3) assumed at redshift slightly below that of S2.

5. Discussion

5.1. Mass distribution in the MS 2137-2353 core

Figure 2 summarizes the mass parameter predictions provided by the fit of the two arcs systems in the HST image. To reproduce the arc system (A0, A2 and A4) a flat density profile is required ($\beta < 0.85$), while the presence of the radial arc very near to the mass center implies a very small core radius ($r_c \leq$3.5 for β=0.8). The only possibility to fit the radial arc with a β=1 profile implies large ellipticities ($\epsilon > 0.22$) and gives highly inconsistent source reconstruction from the 4 image (A01, A02, A2 and A4) system (SSP$\geq$0.81). This mass profile for the MS 2137-2353 core can be rejected at a 8σ level.

This analysis provides a considerable reduction of the available volume of the space of parameters which can fit the arc observations, especially when compared to results based on ground-based observations (see Figure 2). The solution found by Mellier et al (1993) (β=1 and r_c=7") is inconsistent with both arc systems. This is simply related to the fact that, from the ground, the radial arc was found far less extended towards the mass center than in the HST image, and that no morphological information can be obtained from unresolved arcs. The range of parameters which provide reasonable fit of the two arc systems are $0.6 < \beta < 0.85$, $0.06 < \epsilon < 0.18$ and $r_c < 4$". It is likely that the available range for the parameter is even smaller, if one assumes that the ellipticity of the dark matter matches well the ellipticity of both the visible and X-ray matter ($0.12 < \epsilon < 0.17$). If true, the range of mass parameters (described in Figure 2 by a shaded area) is: β =0.78 $\pm$0.05, ϵ = 0.145 $\pm$0.025 and $r_c < 4$" (or $22.5 h_{50}^{-1}$ kpc).

For this range of parameters the expected fifth image of the (A01, A02, A2 and A4) system is predicted overfocused (amplification factor < 1), in agreement with the observations (Figure 1). This analysis does not depend on to the (unknown) redshift of the source, since we have treated the mass (σ^2) in the lensing equation as proportional to D_s/D_{ds}, where D_s and D_{ds} are the angular diameter distance of the source, and from the lens to the source, respectively.

5.2. Properties of the sources

Since the available range of mass parameters is well constrained, one can derive the properties of the source (e.g. luminosity and size) with an unprecedented accuracy. The magnification factor is known with an accuracy of better than 15% for both arc systems.

The arcs A2 and A4 are images of the same source (S1) which is magnified by 13±1.5 and by 9.2±1.0, respectively. This implies that the unlensed source (S1) of the (A0, A2 and A4) system would appear as a R=26.0±0.25 galaxy, a substantial fraction of the uncertainty being related to photometric measurement errors. The corresponding magnification factors for the arcs A01 and A02 reach very high values (46±8). We believe rather unsecure the derivation of redshift information for an object with such a flat spectral energy distribution ($B-R$= 0.4 from Fort et al, 1992). Such colors, as well as the absence of emission line in the optical spectrum could be associated with any intrinsically blue galaxy with 0.8 < z < 2.5, a rather usual range for R=26 galaxies. As a whole, the source has an axis ratio of 1.7 and is rather compact, with a major axis of 0".90±0.05, which corresponds to $7.1{\pm}0.2h_{50}^{-1}$ kpc after accounting for uncertainties related to the magnification factor and to the redshift undetermination. Its morphology shows some resemblance with the reconstructed source of Cl 0024+1654 arc system (Colley et al, 1996), although it is far more complex. Among the 600 local galaxies taken from the compilation of the Color Atlas of Galaxies (Wray,

1988), eight galaxies show some morphological similarities with the source of the (A0, A2 and A4) system, and are by decreasing order of resemblance, NGC 4038, 4618, 0337, 1385, 3256, 6221, 1559 and 3162. Latter have type ranging from T=6 to T=9, and U-V color from 0.25 to 0.6. 3 of them are young irregular systems, 2 shows irregularities because of dust, 2 (including NGC 4038) are the result of galaxy interactions, and the remaining one has a barred spiral morphology. There is little doubt that S1 is a rather young and irregular system at high redshift, while there are some possibilities that either dust or close interaction between two galaxies are contributing to its appearence. The source brightest knot (on top right of the reconstructed source, see Figure 3) is probably an HII region, since the F702W filter corresponds to ultraviolet light in the rest-frame source. It is apparently unresolved in arc A2 and A4, while the large magnification factors in arcs A01 and A02 resolve it into two small elements separated by 0".26 (Figure 1), which correspond to 0".015, or $120h_{50}^{-1}$ pc in the actual source. The gravitational microscope can also provide us detailed informations on the size of the bright and giant HII regions in distant star forming galaxies.

The unlensed source (S2) of the (A5 and AR) system would appear as a R=23.9±0.2 galaxy which resembles to a nearly edge-on barred spiral (Figure 3). The lensing model predicts a very similar redshift for the sources (S1 and S2) of the two arcs systems ($\Delta z \leq 0.03$ at z=1). The (unlensed) projected distance between the two sources is 3".2±0".3, which corresponds to $26 \pm 3 h_{50}^{-1}$ kpc, the error bar accounting for the uncertainties related to the modelling and to the undetermination of the source redshifts. Assuming that A5 is actually related to the source (S3) of the bright knot above AR would imply that 3 sources with similar redshift are within the large magnification area which has a radius smaller than 2" (Figure 3). They might be either interacting galaxies or the result of projection of galaxies lying in a large structure of galaxies.

6. Conclusion

A very simple mass distribution for the dark matter accounts for most of the detailed lensing properties of the two arc systems found in the core of MS 2137-2353, after careful analysis of a deep HST image of the cluster. Within 33 to $150 h_{50}^{-1}$ kpc from the mass center, the major axis and ellipticity of the dark matter component are in a good agreement with those derived from X-ray and visible light, while the dark matter density profile has a slope (β=0.78$\pm$0.05) much flatter than the visible light (β=1.6). MS 2137-2353 is probably a good example of an essentially relaxed cluster at z=0.313, with an increasing mass to light ratio from the very center to r$\sim$ $150 h_{50}^{-1}$ kpc. The mass distribution profile should be associated with a very small or a null core radius ($r_c \leq 22.5 h_{50}^{-1}$ kpc), and could be associated with a single power law, $\rho \sim r^{-1.56\pm0.1}$ within a $150 h_{50}^{-1}$ kpc radius from the cluster center. This could be in agreement with the universal profile predicted by standard CDM simulations (Navarro et al, 1995; Tormen et al, 1996). This analysis also brings some support to the very simple analysis of a large number of arc systems by Wu and Fang (1996) who found a similar value for the slope on average, although they have neglected the effect of subclustering.

The relatively low value for the slope of the cluster mass density profile implies large magnification factors, and provide us with the opportunity to look at details as small as 0".02 in the reconstructed sources. The two sources associated with the two arc systems in the MS 2137-2353 core are very close in redshift space and might be interacting objects. While they are high redshift galaxies (0.8 < z < 2.5), they both have morphologies which are not so unusual compared to that of present-day galaxies. One could be a nearly edge-on barred spiral, the other has a more irregular morphology, which combined with its blue color, suggests a young star-forming system in a closely interacting pair possibly affected by dust. Both sources also show strong peaks of emission, well off their centers, which are

likely associated with HII regions, and hence indicate star formation. Magnification factors in giant arcs can reach so large values that HII regions can be spatially resolved by this technique.

We thank M. C. Willaime for her help in writing the code AIGLE, X.P. Wu for comments on the manuscript and B. Monart for her help in comparing the arc source morphology to those of local ones. This work has received partial financial support from NASA-STScI grant GO-5402.01-93A, NASA grants NAG5-2594 and NAG5-2914.

REFERENCES

Bartelmann, M., 1996 A&A, submitted

Bourassa, R. and Kantowski, R., 1975, ApJ, 195, 13

Colley, W., Tyson, A., Turner, E., 1996, ApJ, 461, L83

Fort, B., Le Fèvre, O., Hammer, F., Cailloux, M., 1992, ApJ, 399, L125

Fort, B. and Mellier, Y., 1994, Astron. Astrophys. Review, 5, 239

Gioia, I. et al, 1996a, ApJ, in preparation

Gioia, I., Shaya, E., Luppino, G., Le Fèvre, O., Hammer, F., Falco, E., 1996b, ApJ, submitted

Hammer, F., 1991, ApJ, 383, 66

Hammer, F. and Rigaut, F., 1989, A&A, 226, 45

Mellier, Y., Fort, B., Kneib, J.P., 1993, ApJ, 407, 33

Navarro, J.F., Frenk, C., White, S., 1995, MNRAS, 275, 720

Schramm, T., 1990, A&A, 231, 19.

Schramm, T. and Kayser, R., 1987, A&A, 174, 361

Tormen, G., Bouchet, F., White, S., 1996, MNRAS, submitted

Wallington, S., Kochanek, K., Koo, D., 1995, ApJ, 448, 51

Wray, J., 1988, "The Color Atlas of Galaxies", Cambridge University Press

Wu, X.P. and Hammer, F., 1993, MNRAS, 262, 187

Wu, X.P. and Fang, L.Z., 1996, ApJ, 467, L45

This manuscript was prepared with the AAS LaTeX macros v4.0.

Fig. 1.— (top): MS 2137-2353 core after subtraction of G1 and G7 galaxies. The subtraction of G7 reveals the complex structure of the bottom-right part of the giant arc A0. Arc images are labelled as in Fort et al (1992). The giant arc is made by the blend of two images (A01 and A02) of the source (S1), also associated with arcs A2 and A4. No extra image is seen near the cluster center. The other arc system is made by the radial arc (AR) and A6 (source S2). The radial arc extends very close to the cluster center (3".4). There is also another possible radial arc indicated as ARN. (bottom): reconstruction of the arcs assuming two sources (S1 and S2) at nearly the same redshift (see text), for a model with β=0.8, r_c=2" and ϵ=0.151. Most of the morphological details are well reproduced, with the noticeable exceptions of the left end of the arc A01 and of the bright knot above the radial arc. Latter is probably related to A5 (source S3). The fifth image of the arc system (A0, A2 and A4) is predicted too faint (near the cross which indicates the mass center), to be detected in the HST image. (box in the top right): zoom of the brigthness knot in A01 and A02, respectively. While this knot is unresolved in A2 and in A4, the extremely large magnification factor in the giant arc allows to resolve it in two sub-knots (SK1 and SK2) in the two images. Note that it is consistent with the fact that A01 and A02 are reversed images (the brightest pixel is found in SK1 in both images). The separation between the two sub-knots is 0".26 which correspond to 0".015 in the unlensed source.

Fig. 2.— The (r_c, ϵ) fundamental plane of mass parameters. Each point corresponds to a fit within 1 pixel accuracy of the brightest knot in arcs A01, A02, A2 and A4. The values of the self consistency parameter (SSP) are indicated near each points. Solid lines connect the points for constant β. Dotted line delimits the area (indicated by arrows) of parameters which fit the location of the radial arc. It has been empirically determined from systematic tests for each set of parameters. Shaded area is the most likely area for the mass parameters, assuming that the ellipticity of the dark matter component matches those of the X-ray and visible matter.

Fig. 3.— The four top panels show the reconstructed source images (RSIs) corresponding to arcs A2, A4, A01 and A02, respectively (from the left to the right and from top to bottom). The corresponding reconstructed source (S1) is the combination of these four RSIs, after re-scaling the intensities, and is shown just below the four top panels. The lowest panel shows the reconstructed sources (S2 and S3, from left to right) of arcs A6 and AR, and of A5 and the bright knot above the radial arc (AR). In the box at the bottom right are displayed the model predicted locations of the sources (S1, S2 and S3) if there were no foreground lensing cluster on their line of sight. Size of the box is 4".

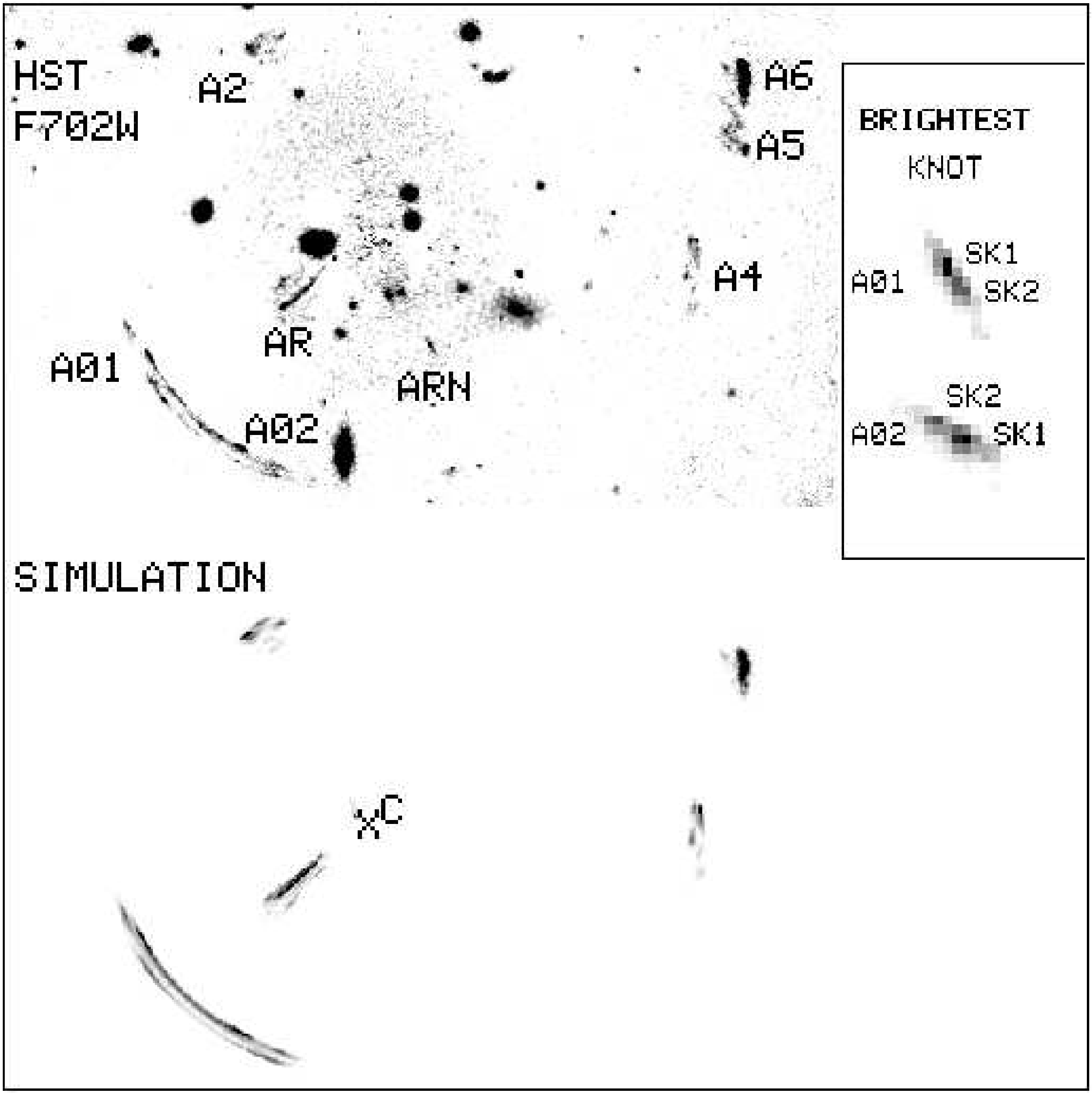
HST
F702W
A2
A6
A5
BRIGHTEST
KNOT
SK1
A01
SK2
A4
AR
A01
ARN
SK2
A02
A02
SK1
SIMULATION
C

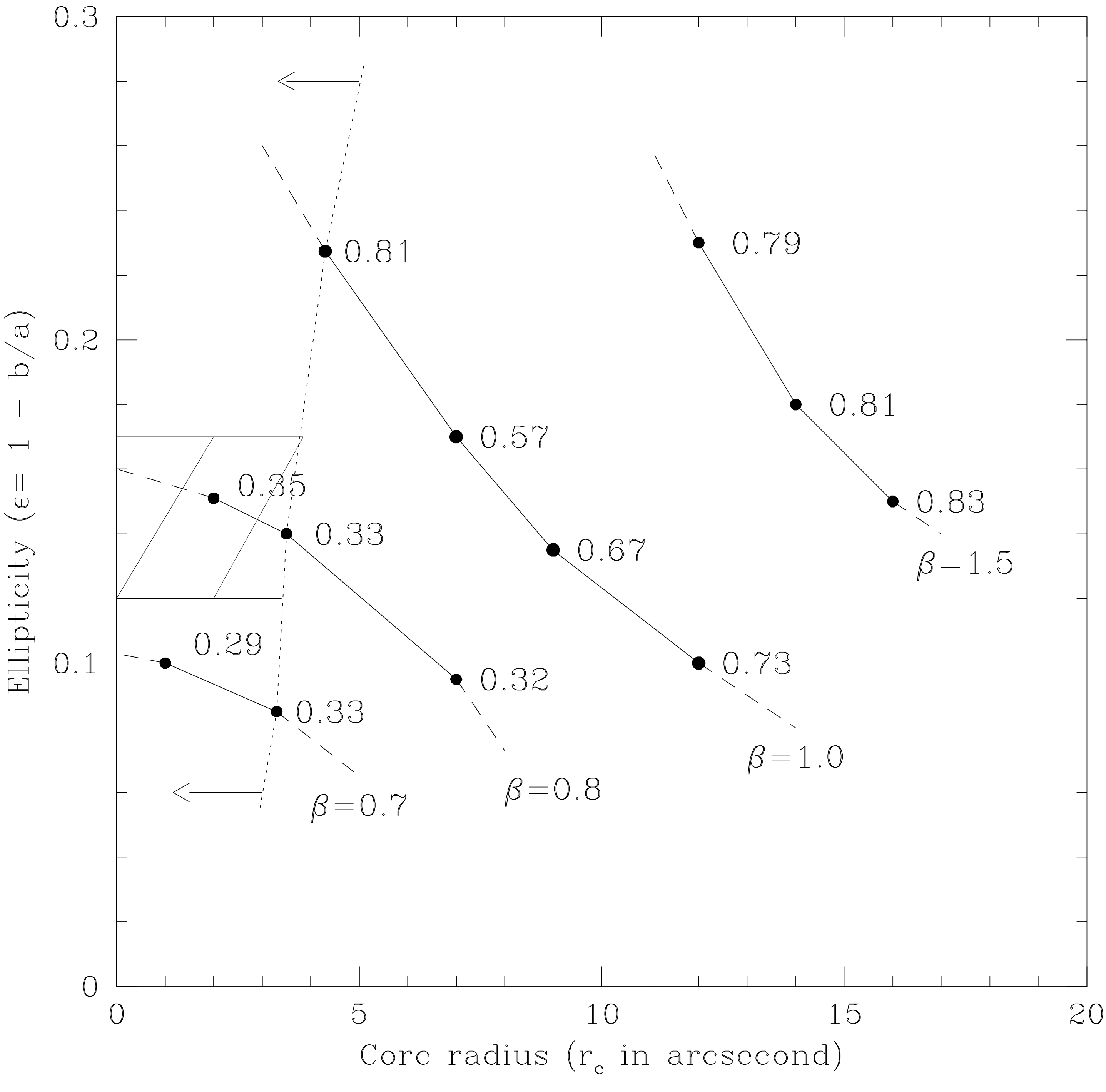

0.3
0.2
0.1
0
0
5
10
15
20
Ellipticity (ϵ= 1 − b/a)
Core radius (r_c in arcsecond)
0.81
0.57
0.67
0.73
0.79
0.81
0.83
0.35
0.33
0.32
0.29
0.33
β=0.7
β=0.8
β=1.0
β=1.5